ACS Medicinal Chemistry Letters

pubs.acs.org/acsmedchemlett

# Computational Modeling of Kinase Inhibitor Selectivity

Govindan Subramanian*,† and Manish Sud‡

†Structure, Design and Informatics, sanofi-aventis U.S., 1041 Route 202-206, P.O. Box 6800, Bridgewater, New Jersey 08807, and ‡MayaChemTools, 4411 Cather Avenue, San Diego, California 92122

**ABSTRACT** An exhaustive computational exercise on a comprehensive set of 15 therapeutic kinase inhibitors was undertaken to identify as to which compounds hit which kinase off-targets in the human kinome. Although the kinase selectivity propensity of each inhibitor against ~480 kinase targets is predicted, we compared our predictions to ~280 kinase targets for which consistent experimental data are available and demonstrate an overall average prediction accuracy and specificity of ~90%. A comparison of the predictions was extended to an additional ~60 kinases for sorafenib and sunitinib as new experimental data were reported recently with similar prediction accuracy. The successful predictive capabilities allowed us to propose predictions on the remaining kinome targets in an effort to repurpose known kinase inhibitors to these new kinase targets that could hold therapeutic potential.

**KEYWORDS** Kinase selectivity, kinase conformation, binding hot spots, computational prediction, binding site signature, kinase inhibitors

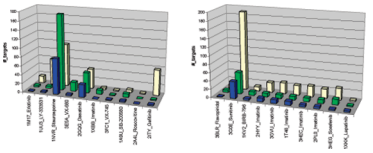

Identifying and understanding small molecule kinase inhibitor selectivity is a major challenge in advancing potent kinase compounds to becoming drugs.[1,2] Given the large human kinome landscape, it is rather difficult to profile very potent or early development/clinical compounds across the ~500 targets[3] to gain upfront knowledge on kinase specificity with the additional fact that not all kinases could be screened in vitro. Small molecule kinase inhibitor selectivity insights are usually gained by pursuing experimental verifications on a representative or a comprehensive subset of the kinase off-targets.[4−8] Although the merits and limitations of the selectivity screening paradigm could be debated, they are often supposed to provide reasonable knowledge and guidance enabling compound prioritization in the decision tree.

In recent years, several computational approaches are being reported in the literature to either complement the experimental findings or to predict the overall kinase off-target activity profiles.[9−20] These approaches primarily overcome the drawbacks of the one-dimensional sequence-based comparison or kinase phylogeny that has been shown to have limited predictive capabilities.[21−23] Very recently, Sheridan et al.[24] reported a two-dimensional quantitative structure−activity relationship (QSAR)-based modeling approach to predict the kinase inhibitor binding profiles on ~160 unique kinases from the Karaman et al. experimental data set[25] along with other experimental data sets. Their approach is based on several physicochemical properties of the 29 residues surrounding the ATP binding site and assumes that all inhibitors occupy the whole ATP binding site. For instance, small molecules like imatinib that predominantly occupy the "base" subsite and not the "sugar" or "phosphate" subsite should be differentiated from ligands like staurosporine that occupy nearly all or most other subpockets of the ATP binding site, and their binding contributions need to be treated differently.

Several years ago, Sheinerman et al. developed the "binding site signature (BSS)" computational approach[26] that uses the three-dimensional (3D) X-ray structural information of a kinase−inhibitor complex to predict the small molecule's off-target kinase activity or potential selectivity profile. In this letter, the application of this approach to predict the selectivity propensity of a given inhibitor against each of the ~480 members of the human kinome is presented. Unlike several other methods mentioned earlier,[9−20] the present 3D approach takes into account most of the residues that make energetically quantifiable contact ("hot spot" residues) with the ligand. This greatly removes the inherent bias involved when considering residues that are part of the ATP binding site irrespective of the occupancy of the ligand in that particular subpocket.

To provide a reasonable validation for the approach, the literature was surveyed to collect experimental data sets for inhibitors that have been cocrystallized with the kinase target and also evaluated systematically against a large kinase panel. This resulted in the identification of one data set reported by Karaman et al. consisting of 38 kinase inhibitors screened on more than 280 unique human kinases providing a complete 280 × 38 matrix of the kinase-compound activity or selectivity space.[25] Among the 38 kinase inhibitors, the 3D structure of the inhibitor bound

**Received Date:** May 11, 2010
**Accepted Date:** July 26, 2010
**Published on Web Date:** July 28, 2010





DOI: 10.1021/ml1001097 | *ACS Med. Chem. Lett.* **2010**, *1*, 395–399

**Table 1.** Summary of the Key Experimental Findings and Prediction Results for the Kinase Inhibitors under Investigation

| PDB ID | kinase conf. | inhibitor | X-ray target[b] | $K_d$ x-ray[c] | $K_d$ best[d] | best target[e] | accuracy[f] | sensitivity[g] | specificity[h] |
|---|---|---|---|---|---|---|---|---|---|
| 1KV2 | DFG-out | BIRB-796 | P38A | 0.37 | 0.37 | P38A | 0.96 | 0.44 | 0.98 |
| 2GQG | DFG-in | dasatinib | ABL1 | 0.53 | 0.093 | EPHA3 | 0.88 | 0.63 | 0.93 |
| 1M17 | DFG-in | erlotinib | EGFR | 0.67 | 0.67 | EGFR | 0.94 | 0.25 | 0.95 |
| 3BLR[a] | DFG-out | flavopiridol | CDK9 | 6.4 | 6.4 | CDK9 | 0.96 | 0.17 | 0.97 |
| 2ITY | DFG-in | gefitinib | EGFR | 1 | 1 | EGFR | 0.80 | 1 | 0.80 |
| 2HYY | DFG-out | imatinib | ABL1 | 12 | 0.7 | DDR1 | 0.95 | 1 | 0.95 |
| 3GVU | DFG-out | imatinib | ABL2 | 10 | 0.7 | DDR1 | 0.94 | 1 | 0.93 |
| 1T46 | DFG-out | imatinib | cKIT | 14 | 0.7 | DDR1 | 0.95 | 1 | 0.95 |
| 3HEC | DFG-out | imatinib | P38A | NA | 0.7 | DDR1 | 0.91 | 0.56 | 0.92 |
| 2PL0 | DFG-out | imatinib | LCK | 40 | 0.7 | DDR1 | 0.92 | 0.56 | 0.93 |
| 1XBB | DFG-in | imatinib | SYK | NA | 0.7 | DDR1 | 0.95 | 0 | 0.99 |
| 1XKK | DFG-out | lapatinib | EGFR | 2.4 | 2.4 | EGFR | 1 | 1.00 | 1 |
| 1UU3 | DFG-in | LY-333531 | PDK1 | 700 | 2.5 | PRKCQ | 0.79 | 0.60 | 0.79 |
| 2A4L | DFG-in | roscovitine | CDK2 | 3400 | 260 | CSNK1D | 0.99 | | 0.99 |
| 1A9U | DFG-in | SB-203580 | P38A | 12 | 12 | P38A | 0.97 | 0.38 | 0.99 |
| 3HEG | DFG-out | sorafenib | P38A | 370 | 1.5 | DDR1 | 0.87 | 0.21 | 0.91 |
| 1NVR | DFG-in | staurosporine | CHK1 | 3.2 | 0.024 | SLK | 0.62 | 0.47 | 0.86 |
| 3G0E[a] | DFG-out | sunitinib | KIT | 0.37 | 0.075 | PDGFRb | 0.43 | 0.77 | 0.35 |
| 3E5A | DFG-in | VX-680 | AURA | 4.1 | 4 | ABL2 | 0.94 | 0.14 | 1 |
| 3FC1 | DFG-in | VX-745 | P38A | 2.8 | 2.8 | P38A | 1 | 1 | 1 |

[a] The X-ray structure is a mutant kinase. [b] Kinase target in which the inhibitor is bound in the X-ray. [c] Experimental $K_d$ values (nM)[25] for the inhibitor against the X-ray crystallized target. [d] The best experimental $K_d$ value (nM) reported for the inhibitor.[25] [e] The kinase target that exhibited the best $K_d$.[25] [f] Calculated using the (true positives + true negatives)/total no. of kinase targets (i.e., 283). [g] True positives/(true positives + false negatives). [h] True negatives/(true negatives + false positive). NA means experimental $K_d$ data are not determined as the inhibitors exhibit weak activity at a 10 $\mu$M compound screening concentration.[25]

complex was reported for 15 in the PDB, and so, this subset was used in the evaluation of multikinase activity prediction (Table S1 in the Supporting Information). A detailed description of the BSS computational approach and the steps involved in kinase off-target activity prediction had been reported earlier[26] and briefly elaborated in the Supporting Information.

Table 1 provides a summary of the kinase−inhibitor complexes along with the reported activity by Karaman et al.[25] for the cocrystallized inhibitors against the kinase targets. Additionally, the best activity for the inhibitor and its associated target is given to provide guidance when comparing and assessing the computational results. This information is important since predictions based on high-affinity ligand bound cocomplexes are expected to be more reliable.[26] Finally, the conformational state of the kinase as reported in either the source or other literature[27] or interpreted through visual inspection is also tabulated so that the results can be compared uniformly where possible.

For comparing the predictions with experimental results, inhibitors with experimental $K_d \leq 100$ nM are classified as "actives" and the rest tagged as "inactives" (see the Supporting Information, Figure S1, for results obtained using different $K_d$ cutoff values). The predicted off-target "actives" are defined as those kinase targets that possess the same number of "hot spots" with similar residues[26] conserved in the same location in the kinome alignment as those identified for the kinase−inhibitor complex under investigation. It should be pointed out that the residue conservation is defined based on the type of interaction [(non)-polar, electrostatic, etc.] with the inhibitor rather than the actual residue property that is conventionally used. Figure 1 shows the histogram plot for the number of kinase targets observed to be active experimentally (green bars) and predicted to be active computationally (yellow bars) for 20 kinase−inhibitor complexes investigated here (also see Table S2 in the Supporting Information). The results for the active (DFG-in; Figure 1a) and inactive (DFG-out; Figure 1b) kinase conformations are discussed separately.

The ∼90% overall prediction accuracy (recognizing the experimentally "active" and "inactive" correctly) and specificity (recognizing the experimentally "inactive" correctly) for the 10 DFG-in bound inhibitors suggest the prediction results to be comparable with the experiments (Figure 1a). Although a high number of false positives are predicted for LY-333531 and gefitinib, most of the experimental actives are indeed captured. Apart from these two instances, the BSS approach does not overpredict the number of plausible kinase off-target actives for the inhibitors considered in this study. Even for the promiscuous inhibitor like staurosporine, the predictions are quite conservative as compared to the number of experimentally reported active kinase targets. Similarly, the prediction appropriately captures highly selective inhibitors like erlotinib, VX-745, VX-680, and SB-203580 without much loss in mispredictions (Table 1). Among all of the inhibitors considered in this class, roscovitine, by-far, had the weakest best affinity ($K_d \sim 260$ nM; Table 1) reported for CSNK1D and had only 11 dose−response data reported.



DOI: 10.1021/ml1001097 | ACS Med. Chem. Lett. 2010, 1, 395–399

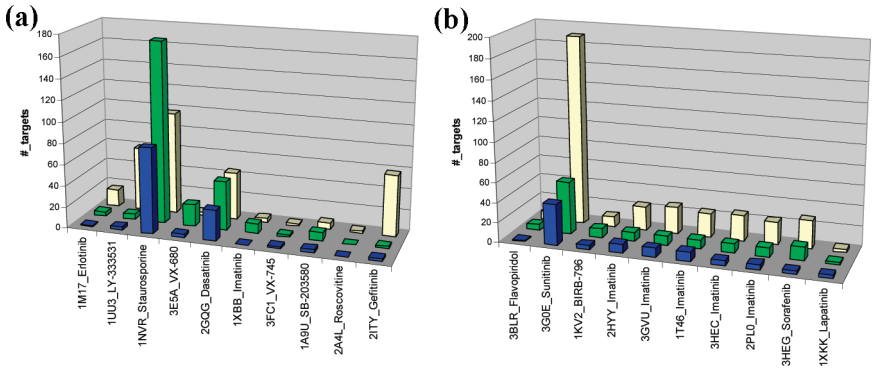


**Figure 1.** Number of kinase targets predicted to be active (yellow), classified as experimentally active ($K_d \leq 100$ nM; green) and the true positives (blue) are shown for kinase inhibitors bound to the DFG-in (a) or DFG-out (b) kinase conformations.

The BSS prediction captures this feature extremely well and suggests the compound to be active against one additional target apart from the cocrystal, which again is a false-positive. This overall prediction success rate clearly provides an advantage in identifying selective kinase inhibitors (if needed) and can reliably distinguish inhibitors that demonstrate broad-spectrum kinase activity.

Figure 1b shows the outcome for the six inhibitors bound to the kinase inactive form. As in the previous cases, the extent of selectivity for a relatively promiscuous inhibitor like sunitinib and a highly selective inhibitor like lapatinib is captured well by the predictions (Table 1). In addition, BIRB-796 and sorafenib, both with good selectivity profiles as indicated by their activities against 9 out of 283 and 15 out of 342 tested kinase targets, are predicted reasonably well (Figure S1 and Table S2 in the Supporting Information).

The consistency in the prediction outcomes when using different kinase−inhibitor cocomplexes as starting points is investigated using imatinib. Figure 1b shows the results for imatinib using ABL1, ABL2, *c*KIT, P38A, and LCK. The inhibitor is bound to the DFG-out conformation in all of the above five kinases with nearly identical binding modes. However, the number of hot spot residues identified in each case varies from 15 to 18 with only nine hot spot residues being common to all of the five X-ray structures (Table S3 in the Supporting Information). In spite of these differences, three of the X-ray starting structures captured the same nine experimentally active kinase targets completely (Figure S1 in the Supporting Information), while the remaining two X-ray structures recovered five out of the nine experimentally active kinase targets successfully. A total of ∼50 unique targets are predicted by the use of the five different X-ray structures (Figure S3 in the Supporting Information). This is reduced to ∼20 targets (minimizing false positives) if a consensus approach is used, and the same is recommended when multiple X-ray structures are available for the same kinase inhibitor. The current predictions also suggest that imatinib would prefer to be bound to the DFG-out conformation in LYN, FYN, SNF1LK, SNF1LK2, STK36, and YES1 kinases as the predictions are consistent across the five DFG-out X-ray targets used in this study (Figure S3 in the Supporting Information). This clearly highlights the advantage on the use of the current approach over those reported in the literature in identifying inhibitors that are bound to either of the two possible kinase conformations.

In the case of imatinib, the inhibitor is bound exactly the same way and in the same position (nearly superimposable) in all of the five different X-ray cocomplexes; hence, the results are consistent. However, caution should be exercised when extrapolating these observations universally against other known kinase inhibitors bound to several kinases and where the inhibitor may be bound slightly differently in the different cocomplexes (based on unpublished results for sorafenib). The current approach assumes that the inhibitor is bound exactly the same way and in the same orientation in all of the kinase targets. However, the plasticity of the binding site residues and side chain flexibility that allows for better/worse interactions with the inhibitor is not captured using a single X-ray cocomplex as reference for the whole kinome.

The average overall prediction accuracy and specificity of ∼90% showcase the successful application of the BSS approach in predicting the kinase inhibitor selectivity map against a majority of the human kinome targets (Table S2 in the Supporting Information). The prediction results are also relatively insensitive to other type of cutoff thresholds used to classify the experimental activity (Figure S1 in the Supporting Information). To our knowledge, this is the first time in the literature where a systematic one-to-one comparison of experiments and predictions are reported for the majority of the human kinome targets. Unlike a typical QSAR approach, the current paradigm does not use any experimental information for model building or hypothesis generation that could subsequently be used for predictions. We believe the success of the current approach to reside mainly in our ability to treat the microenvironment of the ligand binding appropriately. The hot spots are identified through quantitative evaluation of the residue-based contribution to the binding energetics and its breakdown to their corresponding electrostatic and (non)-polar components as well as using the above interaction type to arrive at residue conservation profiles across the other residues in the same position in the kinome alignment.[26] Further analysis of the hot spot residues, especially for sunitinib and gefitinib, show that the current procedure identified binding site residues that are also hit by most of the inhibitors considered here (Table S4 in the Supporting Information). This partially explains the



DOI: 10.1021/ml1001097 | *ACS Med. Chem. Lett.* **2010**, *1*, 395–399

overprediction of the "active" kinase targets as no ligand specific/selective residues were identified as a binding hot spot.

By identifying it as a hot spot for most of the inhibitors studied here, the present result re-emphasizes the relevance of the key gate-keeper residue reported in literature[2,28] (Table S4 in the Supporting Information). The identified hot spot residues also reveal that there are very few residues that are consistently hit by all of the inhibitors, and the majority of the ligands see the surrounding residues differently, albeit occupying the ATP binding site. In addition, the present study clearly demonstrates that there are several energetically important binding site residues apart from the six residues (gate-keeper, two from hinge, and three from glycine-rich loop) that Sheridan et al.[24] identify to be important for the Karaman et al.[25] data set used in their investigation. For example, ≥10 binding hot spots are identified for the inhibitors bound to the inactive kinase conformation (except sunitinib) with several of them not identified in Sheridan et al. study[24] (Table S4 in the Supporting Information).

While all of the inhibitors considered in this study were compared against the 283 kinases for which consistent experimental data were available,[25] a recent study by the same group expanded the number of kinases to 359 and updated the results for sunitinib and sorafenib.[29] Among this set, 59 additional targets could be mapped reliably to the kinome alignment. The predictions were able to capture 6/12 kinase targets (CHEK2, IRAK, MAP3K2, ULK1, ULK3, and YSK4) successfully for sunitinib. Sorafenib, on the other hand, was inactive against 58 of the additional 59 targets, and the predictions captured all of the inactives correctly. This success allows us to propose the screening of the other inhibitors considered in this study against only a subpanel of the additional 59 kinases for which the predictions are positive (Table S5 in the Supporting Information). For instance, erlotinib, flavopiridol, VX-680, VX-745, and lapatinib are predicted to be inactive against all of the 59 additional targets, while a Ser/Thr-kinase like QSK (or SIK3) would be potently inhibited by LY-333531, dasatinib, imatinib, SB-203580, and gefitinib. Indeed, a very recent publication from a different group indicates dasatinib to interact with QSK,[30] providing additional impetus for verifying the other predictions.

Predictions that demonstrate decent correlations to already known experimental findings enable new target(s) identification for existing inhibitors or alternatively help in repurposing known inhibitor(s) based on the validated therapeutic potential for new kinase target(s). Prospectively, we provide the predictions for the 15 kinase inhibitors on ∼150 targets for which experimental $K_d$ values are still unavailable (Table S6 in the Supporting Information). Several of these kinases do not have small molecule kinase inhibitors reported in the literature, and the inhibitors pursued in this study could serve as tool compounds for investigating these kinases.[31]

In summary, the BSS approach has been successfully validated using a consistent experimental data set enabling this semiautomated modeling procedure to be routinely used in a discovery setting for the prediction of potential kinase inhibitor selectivity using the kinase cocrystallized inhibitors. The automation achieved in this in silico workflow allows rapid evaluation of kinase off-target activity against a large number of cocrystallized kinase inhibitors. The procedure is also able to reliably predict the selectivity profile of promiscuous kinase inhibitors like staurosporine and highly selective inhibitors like lapatinib (Figure 1) and to distinguish the selectivity profiles for inhibitors bound to either the DFG-in or the DFG-out kinase conformation with similar accuracies. The overall ∼90% prediction accuracy and specificity reflect the decent statistical outcome achieved through the current modeling procedure.

The successful development of small molecule kinase inhibitors hinges on identifying suitable ligands that exhibit activity against a select combination of kinases[2,32] relevant to the disease mechanism/network. By successfully validating the current approach with extensive experimental data and one-on-one comparison across the majority of the human kinome targets, well-validated computational tools are now available to facilitate the identification of inhibitors, demonstrating targeted multikinase inhibition profile.[33] Indirectly, the current approach also strives to potentially remove targeting undesirable kinases that could later on manifest in clinical attrition.[34]

## SUPPORTING INFORMATION AVAILABLE

Comparison of experimental and predicted data along with the new kinase targets prediction for inhibitors with no experimental data and a brief description of the method and the sequences used, along with the structures of the kinase inhibitors considered in this study. This material is available free of charge via the Internet at http://pubs.acs.org.

## AUTHOR INFORMATION

**Corresponding Author:** *To whom correspondence should be addressed. Tel: 908-231-3618. Fax: 908-231-2492. E-mail: govindan.subramanian@sanofi-aventis.com.

## ACKNOWLEDGMENT

We thank Jean-Marie Bernassau, Peter Monecke, Roy Vaz, and Stephan Reiling for critical suggestions and Sam Billakanti for providing the infrastructure to perform the work. G.S. also thanks Patrick Zarrinkar from Ambit Biosciences for providing the experimental results in a machine-readable form. We also thank the anonymous reviewers for the valuable suggestions to improve the manuscript quality.

## REFERENCES

(1) Sawa, M. Strategies for the design of selective protein kinase inhibitors. *Mini Rev. Med. Chem.* **2008,** *8*, 1291–1297.
(2) Morphy, R. Selectively nonselective kinase inhibition: Striking the right balance. *J. Med. Chem.* **2010,** *53*, 1413–1437.
(3) Manning, G.; Whyte, D. B.; Martinez, R.; Hunter, T.; Sudarsanam, S. The protein kinase complement of the human genome. *Science* **2002,** *298*, 1912–1934.
(4) Melnick, J. S.; Janes, J.; Kim, S.; Chang, J. Y.; Sipes, D. G.; Gunderson, D.; Jarnes, L.; Matzen, J. T.; Garcia, M. E.; Hood, T. L.; Beigi, R.; Xia, G.; Harig, R. A.; Asatryan, H.; Yan, S. F.; Zhou, Y.; Gu, X.-J.; Saadat, A.; Zhou, V.; King, F. J.; Shaw, C. M.; Su, A. I.; Downs, R.; Gray, N. S.; Schultz, P. G.; Warmuth, M.;



DOI: 10.1021/ml1001097 | *ACS Med. Chem. Lett.* **2010,** *1*, 395–399

Caldwell, J. S. An efficient rapid system for profiling the cellular activities of molecular libraries. *Proc. Natl. Acad. Sci. U.S.A.* **2006,** *103*, 3153–3158.
(5) Bain, J.; Cummings, L.; Elliot, M; Shapiro, N.; Hastie, J.; McLauchian, H.; Klevernic, I.; Arthur, S.; Alessi, D.; Cohen, P. The selectivity of protein kinase inhibitors; a further update. *Biochem. J.* **2007,** *48*, 297–315.
(6) Federov, O.; Marsden, B.; Pogacic, V.; Rellos, P.; Muller, S.; Bullock, A. N.; Schwaller, J.; Sundstrom, M.; Knapp, S. A systematic interaction map of validated kinase inhibitors with Ser/Thr kinases. *Proc. Natl. Acad. Sci. U.S.A.* **2007,** *104*, 20523–20528.
(7) Bamborough, P.; Drewry, D.; Harper, G.; Smith, G. K.; Schneider, K. Assessment of chemical coverage of kinome space and its implication for kinase drug discovery. *J. Med. Chem.* **2008,** *51*, 7998–7914.
(8) Goldstein, D. M.; Gray, N. S.; Zarrinkar, P. P. High-throughput kinase profiling as a platform for drug discovery. *Nature Rev. Drug Discovery* **2008,** *7*, 391–397.
(9) Graczyk, P. P. Gini coefficient: A new way to express selectivity of kinase inhibitors against a family of kinases. *J. Med. Chem.* **2007,** *50*, 5773–5779.
(10) Chen, Z.; Zhang, X.; Fernandez, A. Molecular basis for specificity in the druggable kinome: sequence-based analysis. *Bioinformatics* **2007,** *23*, 563–572.
(11) Zahler, S.; Tietze, S.; Totzke, F.; Kubbutat, M.; Meijer, L.; Vollmar, A. M.; Apostolakis, J. Inverse in silico screening for identification of kinase inhibitor targets. *Chem. Biol.* **2007,** *14*, 1207–1214.
(12) Kuhn, D.; Weskamp, N.; Hullermeier, E.; Klebe, G. Functional classification of protein kinase binding sites using Cavbase. *ChemMedChem* **2007,** *2*, 1432–1447.
(13) Sciabola, S.; Stanton, R. V.; Wittkopp, S.; Wildman, S.; Moshinsky, D.; Potluri, S.; Xi, H. Predicting kinase selectivity profiles using Free-Wilson QSAR analysis. *J. Chem. Inf. Model.* **2008,** *48*, 1851–1867.
(14) Sutherland, J. J.; Higgs, R. E.; Watson, I.; Vieth, M. Chemical fragments as foundations for understanding target space and activity prediction. *J. Med. Chem.* **2008,** *51*, 2689–2700.
(15) Caffrey, D. R.; Lunney, E. A.; Moshinsky, D. Prediction of specificity-determining residues for small-molecule kinase inhibitors. *BMC Bioinf.* **2008,** *9*, 491.
(16) Kinnings, S. L.; Jackson, R. M. Binding site similarity analysis for the functional classification of the protein kinase family. *J. Chem. Inf. Model.* **2009,** *49*, 318–329.
(17) Brandt, P.; Jensen, A. J.; Nilsson, J. Small kinase assay panels can provide a measure of selectivity. *Bioorg. Med. Chem. Lett.* **2009,** *19*, 5861–5863.
(18) Vieth, M.; Erickson, J.; Wang, J.; Webster, Y.; Mader, M.; Higgs, R.; Watson, I. Kinase inhibitor data modeling and de novo inhibitor design with fragment approaches. *J. Med. Chem.* **2009,** *52*, 6456–6466 and references therein.
(19) Huang, D.; Zhou, T.; Lafleur, K.; Nevado, C.; Caflisch, A. Kinase selectivity potential for inhibitors targeting the ATP binding site: A network analysis. *Bioinformatics* **2010,** *26*, 198–204.
(20) Cheng, A. C.; Eksterowicz, J.; Geuns-Meyer, S.; Sun, Y. Analysis of kinase inhibitor selectivity using a thermodynamics-based partition index. *J. Med. Chem.* **2010,** *53*, 4502–4510.
(21) Vieth, M.; Higgs, R. E.; Robertson, D. H.; Shapiro, M.; Gragg, E. A.; Hemmerle, H. Kinomics—Structural biology and chemogenomics of kinase inhibitors and targets. *Biochim. Biophys. Acta* **2004,** *1697*, 243–257.
(22) Fabian, M. A.; Biggs, W. H., III; Trieber, D. K.; Atteridge, C. E.; Azimioara, M. D.; Benedetti, M. G.; Carter, T. A.; Ciceri, P.; Edeen, P. T.; Floyd, M.; Ford, J. M.; Galvin, M.; Gerlach, J. L.; Grotzfeld, R. M.; Herrgard, S.; Insko, D. E.; Insko, M. A.; Lai, A. G.; Lelias, J.-M.; Mehta, S. A.; Milanov, Z. V.; Velasco, A. M.; Wodicka, L. M.; Patel, H. K.; Zarrinkar, P. P.; Lockhart, D. J. A small molecule-kinase interaction map for clinical kinase inhibitors. *Nat. Biotechnol.* **2005,** *23*, 329–336.
(23) Vieth, M.; Sutherland, J. J.; Robertson, D. H.; Cambell, R. M. Characterizing the therapeutically validated kinase space. *Drug Discovery Today* **2005,** *10*, 839–846.
(24) Sheridan, R. P.; Nam, K.; Maiorov, V. N.; McMasters, D. R.; Cornell, W. D. QSAR models for predicting the similarity in binding profiles for pairs of protein kinases and the variation of models between experimental data sets. *J. Chem. Inf. Model.* **2009,** *49*, 1974–1985.
(25) Karaman, M. W.; Herrgard, S.; Treiber, D. K.; Gallant, P.; Atteridge, C. E.; Campbell, B. T.; Chan, K. W.; Cicerci, P.; Davis, M. I.; Edeen, P. T.; Faraoni, R.; Floyd, M.; Hunt, J. P.; Lockhart, D. J.; Milanov, Z. V.; Morrison, M. J.; Pallares, G.; Patel, H. K.; Pritchard, S.; Wodicka, L. M.; Zarrinkar, P. P. A quantitative analysis of kinase inhibitor selectivity. *Nat. Biotechnol.* **2008,** *26*, 127–132.
(26) Sheinerman, F. B; Giraud, E.; Laoui, A. High affinity targets of protein kinase inhibitors have similar residues at the positions energetically important for binding. *J. Mol. Biol.* **2005,** *352*, 1134–1156.
(27) Ghose, A. K.; Herbertz, T.; Pippin, D. A.; Salvino, J. M.; Mallamo, J. P. Knowledge based prediction of ligand binding modes and rational inhibitor design for kinase drug discovery. *J. Med. Chem.* **2008,** *51*, 5149–5171.
(28) Zuccotto, F.; Ardini, E.; Casale, E.; Angiolini, M. Through the "gatekeeper door": Exploiting the active kinase conformation. *J. Med. Chem.* **2010,** *53*, 2681–2694.
(29) Zarrinkar, P. P.; Gunawardane, R. N.; Cramer, M. D.; Gardner, M. F.; Bringham, D.; Belli, B.; Karaman, M. W.; Pratz, K. W.; Pallares, G.; Chao, Q.; Sprankle, K. G.; Patel, H. K.; Levis, M.; Armstrong, R. C.; James, J.; Bhagwat, S. S. AC220 is a uniquely potent and selective inhibitor of FLT3 for the treatment of acute myeloid leukemia (AML). *Blood* **2009,** *114*, 2984–2992.
(30) Li, J.; Rix, U.; Fang, B.; Bai, Y.; Edwards, A.; Colinge, J.; Bennett, K. L.; Gao, J.; Song, L.; Eschrich, S.; Superti-Furga, G.; Koomen, J.; Haura, E. B. A chemical and phosphoproteomic characterization of dasatinib action in lung cancer. *Nat. Chem. Biol.* **2010,** *6*, 291–299.
(31) Fedorov, O.; Mueller, S.; Knapp, S. The (un)targeted cancer kinome. *Nat. Chem. Biol.* **2010,** *6*, 166–169.
(32) LoRusso, P. M.; Eder, J. P. Therapeutic potential of novel selective-spectrum kinase inhibitors in oncology. *Expert Opin. Invest. Drugs* **2008,** *17*, 1013–1028.
(33) Knight, Z. A.; Lin, H.; Shokat, K. M. Targeting the cancer kinome through polypharmacology. *Nat. Rev. Cancer* **2010,** *10*, 130–137 and references therein.
(34) Westhouse, R. A. Safety assessment considerations and strategies for targeted small molecule cancer therapeutics in drug discovery. *Toxicol. Pathol.* **2010,** *38*, 165–168.



DOI: 10.1021/ml1001097 | *ACS Med. Chem. Lett.* **2010,** *1*, 395–399